ARTICLE

Co-Self-Assembly of Binary Colloidal Crystals at the Air−Water Interface

Jie Yu, Qingfeng Yan,* and Dezhong Shen

Department of Chemistry, State Key Laboratory of New Ceramics and Fine Processing, Tsinghua University, Beijing 100084, P. R. China

ABSTRACT A simple, fast, and cost-effective co-self-assembly approach to fabricate large-area two-dimensional (2D) binary colloidal crystals has been developed. By manipulating the size ratio and number ratio of the two monodisperse polystyrene latexes, a variety of binary colloidal crystal monolayers with different structures were successfully prepared. The co-self-assembly mechanism of the 2D binary colloidal crystals at the air−water interface was investigated. It was found that the glass slide and the ethanol involved in this work had played significant roles as buffer storage and spreading agent, respectively.

KEYWORDS: self-assembly • binary colloidal crystals • air−water interface

INTRODUCTION

Colloidal crystals with two-dimensional (2D) or three-dimensional (3D) ordered structures of monodisperse colloidal spheres have received a great deal of attention in the past decade because of their practical applications in a wide range of fields, such as photonics (1, 2), catalysis (3), lithography (4, 5), and sensors (6). Binary colloidal crystals could produce a variety of crystal structures that provide a potential route for creating photonic crystals with a full photonic bandgap (7). In addition, they could provide a fascinating model for basic research such as crystallography (8, 9). Hence, it has attracted increasing research interest recently to fabricate binary colloidal crystals.

A number of self-assembly methods have been developed to create binary colloidal crystals. Van Blaaderen and co-workers have reported a layer-by-layer process to grow binary colloidal crystals with stoichiometries of LS, LS_2, and LS_3 by manipulating the size ratio of the small (S) and large (L) spheres as well as the concentration of the colloidal spheres (9). Wang and Möhwald have employed a stepwise spin-coating process to form binary colloidal crystals with various structures depending on the size ratio and the spin speed (10). Zhou et al. have reported the fabrication of binary colloidal crystals by growing a silica colloidal monolayer or multilayer on top of a polystyrene (PS) monolayer using a sequential vertical deposition method (11). By using the confined convective assembly method, Park's group have successfully produced more complicated LS_4 and LS_5 binary colloidal crystal structures by uniformly depositing small spheres on 2D colloidal crystals of large spheres over a large area (12). However, all these approaches were carried out step-by-step, in which a hexagonally close-packed colloidal monolayer or multilayer of large spheres was first prepared on a substrate and used as a template to guide the self-assembly of small spheres. Recently, Li and co-workers described the fabrication of 3D binary colloidal crystals by using one-step self-assembly methods, either by vertical lifting (13) or by inward-growing horizontal deposition (14). By these methods, binary colloidal crystals with various stoichiometric configurations have been obtained. On the other hand, the conventional self-assembly processes often take hours to days to form binary colloidal crystals. For example, Cao and Cong created various array patterns from two kinds of PS colloids by the codeposition method for 8−10 days (8). The low formation speed limits the practical applications of binary colloidal crystals to a great extent. Some efforts have been made to shorten the growth time. Ozin and co-workers (15) reported that it took several hours to prepare binary colloidal crystals with a rich variety of stoichiometries by an accelerated evaporation method. Recently, a rapid self-assembly method with infrared technique assisted has been reported (16). Nevertheless, these approaches rely on special apparatus. Thus, it is highly desired to develop a fast, simple, cost-effective, and single-step method for the preparation of binary colloidal crystals.

Self-assembly of colloidal spheres at the air−water interface is an effective and efficient approach for the fabrication of large-area 2D colloidal crystals (17−19). In this method, latex spheres were spread on the water surface. The interaction forces among the spheres resulted in a well-ordered colloidal crystal monolayer over a large area at the air−water interface. The colloidal crystal monolayer was then transferred to a desired substrate. There are several advantages for this technique. First, this self-assembly process takes only a few seconds which is much faster than the conventional methods. Second, large-area colloidal monolayers can be produced without any special apparatus, and only a small amount of colloidal suspensions is required for each experiment. Finally, the 2D colloidal crystals can be transferred to any kind of substrates regardless of surface wettability and smoothness. However, to the best of our knowledge, this technique has only been used to fabricate monolayers of

* Corresponding author. E-mail: yanqf@mail.tsinghua.edu.cn.
Received for review March 22, 2010 and accepted June 16, 2010

DOI: 10.1021/am100250c

Published on Web 06/28/2010

Table 1. Binary PS Colloids Used in This Study

samples	size of small spheres R_S (nm)	size of large spheres R_L (nm)	size ratio $\gamma_{S/L} = R_S/R_L$	volume fraction ratio $\Phi_{S/L} = \Phi_S/\Phi_L$	number ratio $N_{S/L} = N_S/N_L$
A1	130	887	0.147	0.006	2
A2			0.147	0.013	4
A3			0.147	0.025	8
A4			0.147	0.038	12
B1	173	887	0.195	0.015	2
B2			0.195	0.029	4
B3			0.195	0.059	8
B4			0.195	0.088	12
C1	130	669	0.194	0.015	2
C2			0.194	0.030	4
C3			0.194	0.059	8
C4			0.194	0.089	12

single component but has never been applied to the preparation of 2D binary colloidal crystals.

In this work, we have applied the above air−water interface self-assembly approach to colloidal mixtures and successfully developed a simple, fast and cost-effective method for the fabrication of large-area 2D binary colloidal crystals. The influences of the size ratio and number ratio of the two colloidal spheres on the structures of the binary colloidal crystals were systematically investigated. The co-self-assembly mechanism of the 2D binary colloidal crystals at the air−water interface was also analyzed.

EXPERIMENTAL SECTION

Synthesis of PS Spheres and Preparation of Binary PS Colloids. Monodisperse PS colloidal spheres of 130, 173, 669, and 887 nm in diameter with a polydispersity less than 3% were synthesized using the emulsifier-free polymerization method (20). The PS spheres were washed with water three times by repeated centrifugation and redispersion. Binary PS colloids were obtained by mixing small spheres (130 or 173 nm) and large spheres (669 or 887 nm) in water solvent with different volume fraction ratios (see Table 1) and diluted with the same volume of ethanol.

Fabrication of 2D Binary Colloidal Crystals. Microscopic glass slides with a thickness of 1 mm were cut into pieces. The glass pieces were ultrasonicated in acetone, ethanol, and deionized (DI) water. Then they were boiled in a piranha solution containing concentrated sulfuric acid (96%, Ashland Chemical Inc.) and hydrogen peroxide (30%, Ashland Chemical Inc.) (H_2SO_4:H_2O_2 = 3:1 v/v) for 30 min. (**WARNING!** *The above piranha solution reacts violently with organic materials. Handle with caution.*) After washed with copious DI water, they were dried in nitrogen flow before use. The schematic illustration of the whole process to prepare 2D binary colloidal crystals is demonstrated in Figure 1. A cleaned glass slide was placed in the center of a Petri dish. DI water was then carefully added into the dish to a level where a convex shape was formed around the periphery of the glass slide but without covering the upper surface of the slide (Figure 1a). Ten to twenty microliters of binary colloidal suspension was dropped and spread freely on the glass slide (Figure 1b,c). Once the suspension contacted the surrounding DI water at the edges of glass slide, it was observed that the small and large PS spheres spread on the water surface rapidly and coassembled into 2D arrays in several seconds (Figure 1d). To consolidate the binary colloidal arrays, a drop of 2 wt % dodecylsodiumsulfate (SDS) solution was added to change the water surface tension (Figure 1e). A large-area (more than 2 cm^2) film with iridescent color was observed immediately, which indicated the formation of a large-area binary colloidal crystal monolayer at the air−water surface (Figure 2). To transfer the monolayer to a substrate easily, the liquid level was raised by adding more DI water (Figure 1f). The glass slide inside the Petri dish was then taken out carefully. A desired substrate was inserted beneath the binary colloidal crystal monolayer. The monolayer was then lifted from the water surface as a whole and dried at room temperature (Figure 1g).

Characterization. Field-emission scanning electron microscope (FESEM) images were captured on a Gemini LEO 1530 instrument. The optical photograph of the binary colloidal crystal monolayer at the water−air interface was acquired using a digital camera (Nikon Coolpix3700).

RESULTS AND DISCUSSION

Structures of the Binary Colloidal Crystals. It has been demonstrated that when two types of colloidal spheres with different sizes are mixed together, they can cocrystallize to form binary crystal structures analogous to those seen in atomic systems (21). The structure and stoichiometry of the binary crystals were found to be dependent on the size ratio ($\gamma_{S/L}$) of the two types of spheres and their number ratio ($N_{S/L}$), which can be calculated from the volume fraction ratios ($\Phi_{S/L}$) of the two colloids. In this work, we studied the morphology of binary colloidal crystals from the mixed suspension of large and small PS colloidal spheres with $\gamma_{S/L}$ of 0.147 or 0.195 and $N_{S/L}$ of 2, 4, 8, or 12.

In a given condition, the large spheres self-assembled into ordered arrays. At the same time, the small spheres were co-self-assembled in the interstices of large spheres, forming a monolayer of binary colloidal crystal. The cross-section SEM image of the monolayer was illustrated in Figure S1 in the Supporting Information. There are two kinds of interstices for the arrangement of small spheres, including the 3-fold voids formed by three neighboring large spheres and the channels between two neighboring large spheres. An increase in $N_{S/L}$ led to continued accretion of small spheres occupying the interstices of large spheres, resulting in binary colloidal crystals with complex morphologies. The domain size of the ordered binary colloidal crystal could achieve several tens of square micrometers.

Figure 3 shows the SEM images of sample A1 to A4 containing 130 nm small spheres and 887 nm large spheres

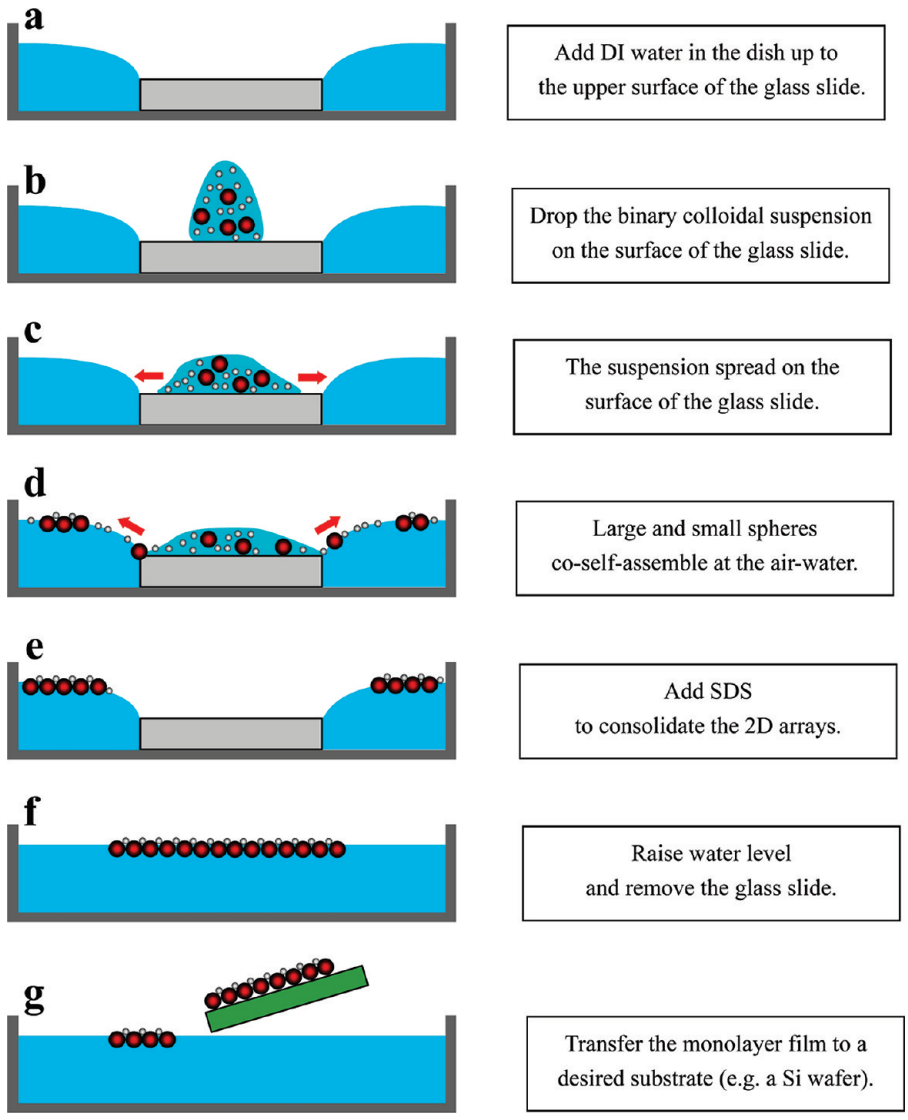

FIGURE 1. Procedure for the fabrication of 2D binary colloidal crystals at the air–water interface.

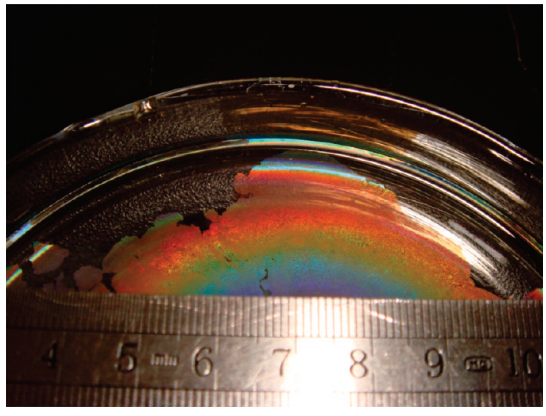

FIGURE 2. Photograph of a large-area binary colloidal crystals showing iridescent color at the air–water interface.

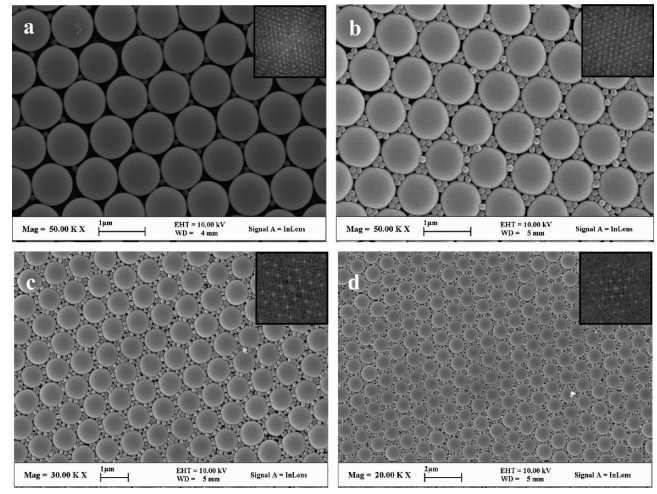

FIGURE 3. SEM images of binary colloidal crystals of large (R_L = 887 nm) and small (R_S = 130 nm) spheres with (a) $\gamma_{S/L}$ = 0.147, $N_{S/L}$ = 2; (b) $\gamma_{S/L}$ = 0.147, $N_{S/L}$ = 4; (c) $\gamma_{S/L}$ = 0.147, $N_{S/L}$ = 8; and (d) $\gamma_{S/L}$ = 0.147, $N_{S/L}$ = 12. The insets are the corresponding 2D FFT images.

with $\gamma_{S/L} = 0.147$ and $N_{S/L}$ values ranging from 2 to 12. Figure 3a shows the structure of sample A1 ($\gamma_{S/L} = 0.147$, $N_{S/L} = 2$). It can be seen that single small spheres are localized in the 3-fold voids, forming an LS_2 binary colloidal crystal. In this case, the most common type of defect is the vacancies formed in the 3-fold voids without small spheres filling. This result is in accordance with the theoretical model, i.e., if $\gamma_{S/L} < 0.15$, the small spheres could freely flow other than fix in

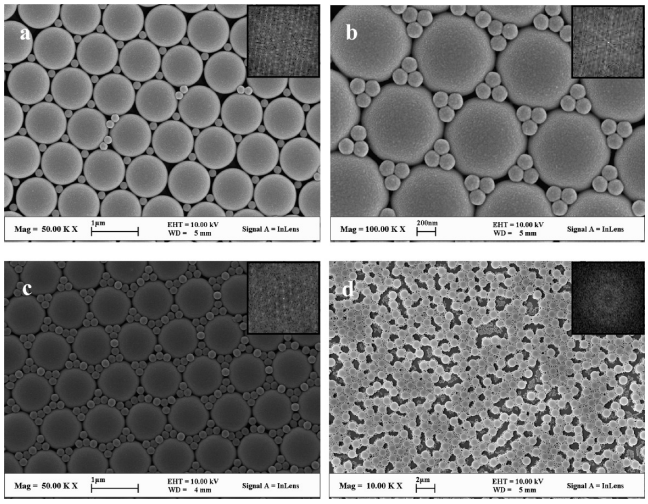

FIGURE 4. SEM images of binary colloidal crystals of large (R_L = 887 nm) and small (R_S = 173 nm) spheres with (a) $\gamma_{S/L}$ = 0.195, $N_{S/L}$ = 2; (b) $\gamma_{S/L}$ = 0.195, $N_{S/L}$ = 4; (c) $\gamma_{S/L}$ = 0.195, $N_{S/L}$ = 8; and (d) $\gamma_{S/L}$ = 0.195, $N_{S/L}$ = 12. The insets are the corresponding 2D FFT images.

the voids (22). Upon increasing $N_{S/L}$ from 2 to 4, the number of small spheres occupying the 3-fold voids increases from one to three, as shown in Figure 3b. Each large sphere is approximately surrounded by 6 small spheres, forming a binary colloidal crystal with stoichiometry of LS_6. When the concentration of small spheres increases to $N_{S/L}$ = 8, there are a greater number of small spheres surrounding the large ones and filling in all 3-fold voids as well as the channels (Figure 3c). For sample A4, when the number ratio $N_{S/L}$ approaches 12, the arrangement of small spheres is still highly ordered in the interstitial sites in most areas (Figure 3d). However, it is observed that both small and large spheres are more close-packed than sample A3.

The SEM images shown in Figure 4 illustrate the structures of sample B1 to B4, which were fabricated from mixtures of 173 nm small spheres and 887 nm large spheres. Similar to sample set A, changing the concentration of small spheres resulted in binary colloidal crystals with different structure. However, for sample B4, when the number ratio $N_{S/L}$ was increased to 12 which was same as that of sample A4, disordered structure was obtained as shown in Figure 4d, rather than the ordered structure formed in sample A4 (Figure 3d). This could be explained by that the structure of the final binary colloidal crystal was determined by a combination effect of the size ratio and the number ratio of two colloids. For a binary system with a given size ratio, when the number ratio exceeds a threshold value, the interstitial sites around large spheres would not be able to provide sufficient space to accommodate all the small spheres. As a result, ordered 2D binary colloidal crystals could not be achieved. For sample B4 with a size ratio of 0.195, when the number ratio was increased to 12, disordered structure was obtained, which implies there was no sufficient space around the large spheres for the small spheres to fill in. However, for sample A4 with a relative smaller size ratio of 0.147, ordered arrangement could still be obtained when the number ratio achieved 12, as observed in Figure 3d. To further prove this point, we increased the number ratio of sample A to 20, and it was found that the crystalline packing of the colloids was hampered (see Figure S2 in the Supporting Information).

The insets in Figures 3 and 4 are the corresponding 2D Fast Fourier Transform (FFT) images of sample set A and B, respectively. The inset images in Figure 3a–d and Figure 4a–c exhibit six-spot patterns, indicating the regular hexagonal closed-packed symmetry of the 2D binary colloidal crystals. However, halo ring pattern in Figure 4d reflects that the disordered structure was obtained.

To demonstrate the validity of this air–water interface method for 2D binary crystals fabrication, we prepared sample set C using 669 nm large spheres and 130 nm small spheres with the same size ratio and number ratio as sample set B. It is observed that the structures of sample set C are similar to the results of set B, as shown in Figure S3 in the Supporting Information. Thus, it could be deducted that this co-self-assembly approach at the air–water surface can be applied to various binary colloidal mixtures. 2D binary colloidal crystals with more complicated structures are expected to be achieved easily by simply adjusting the size ratio and the number ratio of small and large spheres.

When the size ratio $\gamma_{S/L}$ was too large, the ordered packing of the colloid spheres would be hindered. In this work, disordered monolayer was obtained by binary suspensions of 173 nm/669 nm spheres with $\gamma_{S/L}$ = 0.259. It was observed that most of the large spheres were separated by the accumulated small spheres. According to Kitaev's results (15), the unsuccessful formation of ordered 2D binary colloidal crystals in this case could be caused by the electrostatic and entropic forces.

Co-Self-Assembly Mechanism of 2D Binary Colloidal Crystals at the Air–Water Interface. Figure 1 illustrates the procedure to fabricate 2D binary colloidal crystals. In this study, a highly hydrophilic glass substrate was placed inside a Petri dish. DI water was then carefully added into the dish to surround the glass slide (Figure 1a). When the colloidal mixture was dropped onto the glass slide, a convex layer of the colloidal suspension was formed. Because of the hydrophilic nature of the glass surface and the spreading effect of ethanol, the colloidal suspension spread on the glass slide rapidly (Figure 1b). When the colloidal suspension reached the periphery of the glass slide and contacted the surrounding water, colloidal spheres could spread onto the water surface freely. The floating colloidal spheres self-assembled into arrays due to the contribution from the attractive capillary force together with the repulsive electrostatic force (18, 23) (Figure 1c). The addition of surfactant SDS changed the surface tension of water, which facilitated packing the isolated colloidal arrays into large-area highly ordered 2D crystals (Figure 1d).

It was found that if experiments were carried out without a glass slide (e.g., directly drop the colloids onto the water surface or drip the colloids along the inner wall of the dish), it was difficult to form a highly ordered monolayer on the water surface. In this case, it was observed that the colloidal suspension diffused onto the water surface instantaneously, so that there was no sufficient time for nanospheres to approach to

each other and self-assemble into ordered structure. As a result, only sparsely distributed colloidal spheres and clusters were floating on the water surface. Even with the help of SDS, no highly ordered monolayer was obtained. In this study, the glass slide plays a role as buffer storage for the colloidal suspension, which limits the contact area between the suspension and the water to the four boundary edges. Consequently, the spreading speed of the colloids is reduced to a level which provides enough time for the colloidal spheres to self-assemble. In addition, the hydrophilicity of the glass slide is also crucial to the formation of the final ordered 2D crystals. If the glass slide was not highly hydrophilic, the colloidal suspension could not uniformly spread on the slide, which further decreased the ordered range of the 2D arrays and resulted in a disordered monolayer.

In this work, ethanol has played a significant role as a spreading agent (23) during the formation of the 2D binary colloidal crystals. It was found that if the dispersion medium was changed to water only, colloidal crystal monolayer could not be produced even following the same procedure. Without ethanol, when the aqueous colloidal suspension on the glass slide attaches the surrounding water surface, the spreading of the colloids is only a result of the Brownian motion. In this case, the spreading is a quite slow process, which is not helpful for self-assembly of ordered colloidal arrays.

In addition, it was found that the water level would have important influence on the experimental results. If the water level was too low, the water around the glass slide would be pushed away by the approaching colloidal suspension. This is possible because of the relative lower surface tension of the ethanol/water mixture compared with water, which promotes the mixture to replace the surrounding water to wet the Petri dish. In this case, the suspension could not spread onto the water surface, and no assembly process was observed. On the other hand, if too much surrounding water was added so that the curvature of the convex shape exceeded a threshold value, the water would cover the glass slide in the Petri dish, which resulted in a phenomenon the same as dropping the suspension directly onto the water surface.

It is well-known that the attractive capillary force together with other interparticle forces drive the self-assembly of single-component colloidal crystal monolayer at the water−air interface (18, 23). However, for the formation of binary colloidal crystal monolayer, besides these forces, the coeffects of size ratio and number ratio must be considered. Especially, the size ratio and number ratio are of importance in determining the structure of the final 2D binary colloidal crystal. When the large PS spheres self-assembled into a hexagonal close-packed monolayer, they would form interstices which were the most energy favorable positions for self-assembly of the small PS spheres. However, only when the size ratio and number ratio satisfied certain conditions as described in the previous section could the large and small PS spheres in the suspension co-self-assemble into large-area highly ordered 2D binary colloidal crystals at the air−water interface.

SUMMARY

In summary, we have demonstrated the fabrication of large-area 2D binary colloidal crystals by using a co-self-assembly approach at the air−water interface. These 2D binary colloidal crystals can be transferred as a whole onto any kind of solid substrates. The approach is simple and does not rely on any special apparatus. Also, it is fast and the preparation time is shortened from hours to seconds. It is believed that the glass slide and ethanol have played important roles during the formation of highly ordered monolayer. By adjusting the size ratio and number ratio of the two colloids, we have produced binary colloidal crystals with various structures. These large-area 2D binary colloidal crystals may find potential applications in the fields of photonics, solar cells, catalysis, or sensors.

Acknowledgment. This work was supported by the Natural Science Foundation of China (Project 50903046), the Fok Ying Tung Education Foundation (Project 122018), and the Research Fund for the Doctoral Program of Higher Education of China (Project 20090002120043). The authors thank Professor L. Qi and Ms. C. Li from College of Chemistry, Peking University, People's Republic of China, for their valuable discussion.

Supporting Information Available: Cross-section SEM image of a 2D binary colloidal crystal monolayer, SEM image of a binary colloidal crystal of 887 nm large spheres and 130 nm small spheres ($\gamma_{S/L} = 0.147$) with $N_{S/L} = 20$, and SEM images of binary colloidal crystals of 669 nm large spheres and 130 nm small spheres ($\gamma_{S/L} = 0.194$) with different $N_{S/L}$ (2, 4, 8, and 12) (PDF). This material is available free of charge via the Internet at http://pubs.acs.org.

REFERENCES AND NOTES

(1) John, S. *Phys. Rev. Lett.* **1987**, *58*, 2486.
(2) Xia, Y.; Gates, B.; Li, X. Y. *Adv. Mater.* **2001**, *13*, 409.
(3) Velev, O. D.; Tessier, P. M.; Lenhoff, A. M.; Kaler, E. W. *Nature* **1999**, *401*, 548.
(4) Deckman, H. W.; Dunsmuir, J. H. *Appl. Phys. Lett.* **1982**, *41*, 377.
(5) Hulteen, J. C.; Treichel, D. A.; Smith, M. T.; Duval, M. L.; Jensen, T. R.; Duyne, R. P. V. *J. Phys. Chem. B* **1999**, *103*, 3854.
(6) Weissman, J. M.; Sunkara, H. B.; Tse, A. S.; Asher, S. A. *Science* **1996**, *274*, 959.
(7) Wan, Y.; Cai, Z.; Xia, L.; Wang, L.; Li, Y.; Li, Q.; Zhao, X. S. *Mater. Lett.* **2009**, *63*, 2078.
(8) Cong, H.; Cao, W. *J. Phys. Chem. B* **2005**, *109*, 1695.
(9) Velikov, K. P.; Christova, C. G.; Dullens, R. P. A.; van Blaaderen, A. *Science* **2002**, *296*, 106.
(10) Wang, D.; Möhwald, H. *Adv. Mater.* **2004**, *16*, 244.
(11) Zhou, Z.; Yan, Q.; Li, Q.; Zhao, X. S. *Langmuir* **2007**, *23*, 1473.
(12) Kim, M. H.; Im, S. H.; Park, O. O. *Adv. Mater.* **2005**, *17*, 2501.
(13) Wang, J.; Li, Q.; Knoll, W.; Jonas, U. *J. Am. Chem. Soc.* **2006**, *128*, 15606.
(14) Wang, L.; Wan, Y.; Li, Y.; Cai, Z.; Li, H.; Zhao, X. S.; Li, Q. *Langmuir* **2009**, *25*, 6753.
(15) Kitaev, V.; Ozin, G. A. *Adv. Mater.* **2003**, *15*, 75.
(16) Zheng, Z.; Gao, K.; Luo, Y.; Li, D.; Meng, Q.; Wang, Y.; Zhang, D. *J. Am. Chem. Soc.* **2008**, *130*, 9785.
(17) Rybczynski, J.; Ebels, U.; Giersig, M. *Colloids Surf. A* **2003**, *219*, 1.
(18) Retsch, M.; Zhou, Z.; Rivera, S.; Kappl, M.; Zhao, X. S.; Jonas, U.; Li, Q. *Macromol. Chem. Phys.* **2009**, *210*, 230.
(19) Li, C.; Hong, G.; Wang, P.; Yu, D.; Qi, L. *Chem. Mater.* **2009**, *21*, 891.
(20) Shim, S. E.; Cha, Y. J.; Byun, J. M.; Choe, S. *J. Appl. Polym. Sci.* **1999**, *71*, 2259.
(21) Bartlett, P.; Ottewill, R. H.; Pusey, P. N. *Phys. Rev. Lett.* **2004**, *68*, 3801.
(22) Wang, D.; Möhwald, H. *J. Mater. Chem.* **2004**, *14*, 459.
(23) Xia, Y.; Gates, B.; Yin, Y.; Lu, Y. *Adv. Mater.* **2000**, *12*, 693.

AM100250C